Abdominal Radiology (2019) 44:1367–1378
https://doi.org/10.1007/s00261-018-1833-4

TECHNICAL

Differential diagnosis of gallbladder polypoid lesions using contrast-enhanced ultrasound

Haruo Miwa[1] · Kazushi Numata[1] · Kazuya Sugimori[1] · Katsuyuki Sanga[1] · Akane Hirotani[1] · Shun Tezuka[1] · Yoshihiro Goda[1] · Kuniyasu Irie[1] · Tomohiro Ishii[1] · Takashi Kaneko[1] · Katsuaki Tanaka[1] · Shin Maeda[2]

Published online: 26 November 2018

Abstract

Purpose The purpose of the study is to evaluate the utility of contrast-enhanced ultrasound (CEUS) for the differential diagnosis of gallbladder polypoid lesions (GPLs).

Methods Thirty-six patients with GPLs (17 with gallbladder cancer, 19 with benign polyps) who underwent CEUS were enrolled in the study. The mean age of patients was 65.7 ± 12.6 years. Perflubutane-based contrast agent and high-mechanical index mode, which can eliminate the background B-mode and provide precise visualization of tumor vessels, were used for CEUS, and two blinded readers evaluated the images, retrospectively.

Results Patient age and size of malignant GPLs (72.4 ± 9.4 years and 23.4 ± 7.5 mm) were significantly greater than those for benign lesions (59.6 ± 12.3 years and 12.4 ± 2.9 mm) ($P < 0.01$, respectively), and the receiver operating characteristic analysis showed the cut-off value as over 65 years and 16 mm. Univariate analysis showed that heterogeneity in B-mode (80% [12/15]), sessile shape (76% [13/17]), dilated vessel (71% [12/17]), irregular vessel (82% [14/17]), and heterogeneous enhancement (59% [10/17]) on CEUS were significantly correlated with malignant GPLs ($P < 0.01$, respectively). On CEUS, the diagnostic criterion for malignant GPLs was defined as having one or more of the above four features because of the highest accuracy. Sensitivity, specificity, and accuracy for malignant GBLs were 88%, 68%, and 78% for patient age; 76%, 89%, and 83% for size of GPLs; 80%, 68%, and 74% for B-mode; and 94%, 89%, and 92% for CEUS, respectively.

Conclusions CEUS is useful for the differential diagnosis of malignant and benign GPLs.

Keywords Contrast-enhanced ultrasound · Gallbladder cancer · Gallbladder polyp · Sonazoid

Introduction

In its early stages, gallbladder cancer is an asymptomatic disease, and is associated with a poor prognosis if found in an inoperable condition [1]. In contrast to lesions in the stomach or colon, neither endoscopic observation nor forceps biopsy can be performed for gallbladder lesions. Cytology of bile aspirates using endoscopic biliary drainage has low sensitivity [2], and fine-needle aspiration under guidance with endoscopic or transabdominal percutaneous ultrasound (US) carries a risk for dissemination to the abdominal cavity [3]. Therefore, it has become extremely important to improve the accuracy of diagnostic imaging and identify gallbladder cancer at an early stage.

Transabdominal US is usually used to detect gallbladder lesions at screening examinations [4]. Gallbladder polypoid lesions (GPLs) > 10 mm at the largest diameter and sessile shape have been reported as malignancy in several studies [5–8]. However, the need for more accurate diagnostic methods to differentiate malignant GPLs from benign has

✉ Kazushi Numata
kz-numa@urahp.yokohama-cu.ac.jp

[1] Gastroenterological Center, Yokohama City University Medical Center, 4-57 Urafune-cho, Minami-ku, Yokohama, Kanagawa 232-0024, Japan

[2] Division of Gastroenterology, Yokohama City University Graduate School of Medicine, 3-9 Fukuura, Kanazawa-ku, Yokohama, Kanagawa 236-0004, Japan

increased in accordance with the development of US systems able to detect smaller lesions [9, 10].

Presently, there is no established imaging technique for diagnosis of GPL based on hemodynamic aspects. Although color Doppler imaging can visualize vessels in GPL, the ability to detect small vessels for differential diagnosis is insufficient. Additionally, contrast-enhanced computed tomography (CT) is insufficient for evaluating vascularity in GPL, given its limitations in spatial resolution [11]. Contrast-enhanced ultrasound (CEUS) with the perflubutane-based contrast agent, Sonazoid (Daiichi Sankyo, Tokyo, Japan), provides higher spatial resolution and

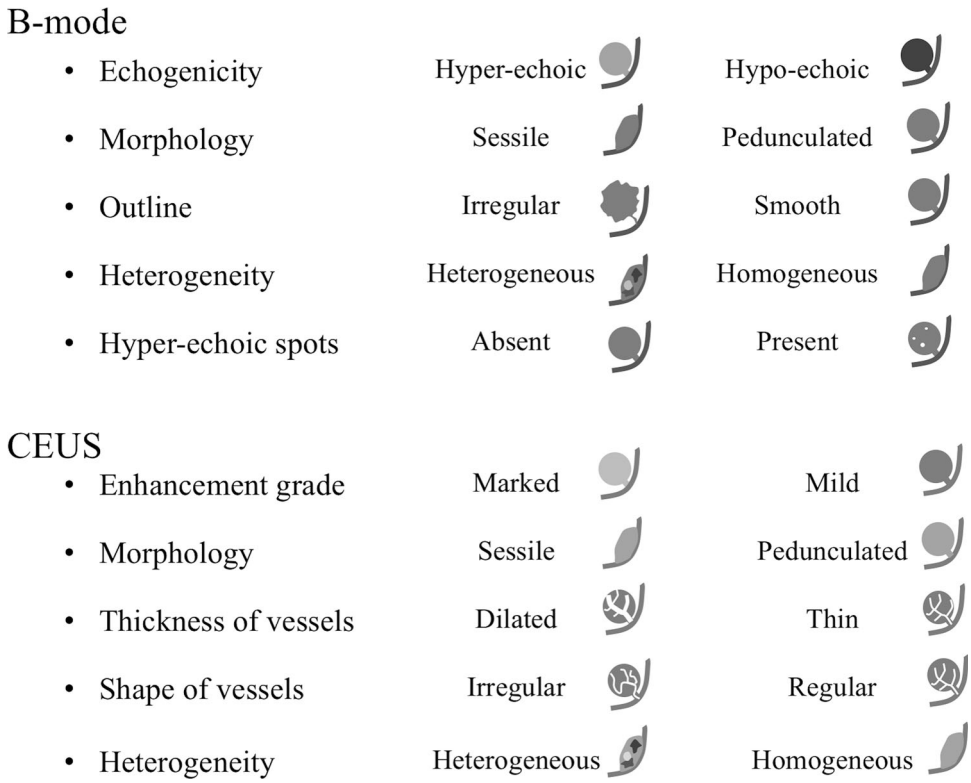

Fig. 1 Evaluation criteria

Table 1 Clinical characteristics of the subjects with GPLs enrolled in this study

	Malignant (N = 17)	Benign (N = 19)	P value
Age [mean ± SD, range (years)]	72.4 ± 9.4, 52–87	59.6 ± 12.3, 34–83	< 0.001[a]
< 65	2	13	
≧ 65	15	6	
Sex			0.739[b]
Male	8	11	
Female	9	8	
Diameter of lesions [mean ± SD, range (mm)]	23.4 ± 7.5, 13–37	12.4 ± 2.9, 10–20	< 0.001[c]
10–20 mm	8	18	
21–40 mm	9	1	
Diagnosis confirmed by			0.002[c]
Surgery	12	11	
Biopsy and cytology	5	0	
Follow-up	0	8	

GPLs Gallbladder polypoid lesions

[a]According to the Student *t*-test

[b]According to the Chi-squared test

[c]According to the Fisher's exact test

real-time evaluation [12]. Previous studies have investigated the utility of CEUS using Sonazoid for characterization of hepatic lesions [13] and pancreatic lesions [14]. For Sonazoid-enhanced US, low-mechanical-index (MI) contrast mode (MI = 0.2–0.3) is usually used to scan the target lesions continuously. However, CEUS images in low-MI settings are difficult to evaluate for hyper-echoic lesions, such as GPLs, due to influence of the echogenicity of background B-mode. Additionally, it cannot depict precise vessel images. Therefore, we use the high-MI contrast mode in CEUS (coded harmonic angio mode [CHA, MI = 0.6–1.2]) to eliminate the echogenicity of the background B-mode, to evaluate vascularity in GPL. This modality is essential for accurate assessment of vascularity in GPLs, especially in cases of hyper-echoic and small lesions in B-mode.

In the present study, we observed the vascularity, including vessels and enhancement, of GPL using CEUS and investigated its ability to differentially diagnose benign and malignant lesions.

Table 2 Findings of GPLs evaluated by two readers

	Reader 1	Reader 2	kappa value
B-mode			
Echogenicity			0.43
Hyperechoic	53 (18/34)	65 (22/34)	
Hypoechoic	47 (16/34)	35 (12/34)	
Morphology			0.64
Sessile	68 (23/34)	53 (18/34)	
Pedunculated	32 (11/34)	47 (16/34)	
Outline			0.49
Irregular	68 (23/34)	76 (26/34)	
Smooth	32 (11/34)	24 (8/34)	
Heterogeneity			0.41
Heterogeneous	47 (16/34)	65 (22/34)	
Homogeneous	53 (18/34)	35 (12/34)	
Hyperechoic spots			0.54
Absent	50 (17/34)	32 (11/34)	
Present	50 (17/34)	68 (23/34)	
CEUS			
Enhancement grade			0.79
Marked	89 (32/36)	69 (25/36)	
Mild	11 (4/36)	31 (11/36)	
Morphology			0.83
Sessile	39 (14/36)	47 (17/36)	
Pedunculated	61 (22/36)	53 (19/36)	
Thickness of vessel			0.71
Dilated vessel	33 (12/36)	42 (15/36)	
Thin vessel	67 (24/36)	58 (21/36)	
Shape of vessels			0.66
Irregular vessel	42 (15/36)	42 (15/36)	
Regular vessel	58 (21/36)	58 (21/36)	
Heterogeneity			0.82
Heterogeneous	36 (13/36)	33 (12/36)	
Homogeneous	64 (23/36)	67 (24/36)	

GPLs Gallbladder polypoid lesions

Data are percentages; data in parentheses are numbers of GPL

Two malignant GPLs were omitted from B-mode images due to sludge

Table 3 Findings of GPLs after consensus meeting

	Malignant (N = 17)	Benign (N = 19)	P value
B-mode			
Echogenicity			0.165[a]
Hyperechoic	40 (6/15)	68 (13/19)	
Hypoechoic	60 (9/15)	32 (6/19)	
Morphology			0.271[b]
Sessile	80 (12/15)	58 (11/19)	
Pedunculated	20 (3/15)	42 (8/19)	
Outline			0.462[b]
Irregular	67 (10/15)	79 (15/19)	
Smooth	33 (5/15)	21 (4/19)	
Heterogeneity			0.007[b]
Heterogeneous	80 (12/15)	32 (6/19)	
Homogeneous	20 (3/15)	68 (13/19)	
Hyperechoic spots			0.630[a]
Absent	47 (7/15)	32 (6/19)	
Present	53 (8/15)	68 (13/19)	
CEUS			
Enhancement grade			1.000[b]
Marked	88 (15/17)	89 (17/19)	
Mild	12 (2/17)	11 (2/19)	
Morphology			< 0.001[b]
Sessile	76 (13/17)	5 (1/19)	
Pedunculated	24 (4/17)	95 (18/19)	
Thickness of vessel			< 0.001[b]
Dilated	71 (12/17)	11 (2/19)	
Thin	29 (5/17)	89 (17/19)	
Shape of vessels			< 0.001[b]
Irregular	82 (14/17)	5 (1/19)	
Regular	18 (3/17)	95 (18/19)	
Heterogeneity			0.001[b]
Heterogeneous	59 (10/17)	5 (1/19)	
Homogeneous	41 (7/17)	95 (18/19)	

GPLs Gallbladder polypoid lesions

Data are percentages; data in parentheses are numbers of GPL

Two malignant GPLs were omitted from B-mode images due to sludge

[a]According to the Chi-squared test

[b]According to the Fisher's exact test

Materials and methods

Patients

Between February 2007 and March 2017, 36 consecutive patients (17 male, 19 female) with GPL $\geq$ 10 mm and $<$ 40 mm in size, who underwent CEUS at the authors' institution were identified. The mean age of patients was 65.7 $\pm$ 12.6 years (range, 34–87). Seventeen patients had malignant and 19 had benign GPLs. Twelve cases of malignant GPLs and 11 cases of benign lesions were treated surgically, and the remaining five malignant GPLs were diagnosed by the pathological results obtained by endosonographic fine-needle aspiration biopsy for lymph node metastasis (n = 2), endoscopic transpapillary bile aspiration cytology (n = 2), or percutaneous biopsy for liver metastasis (n = 1). In these cases, subsequent clinical course and images evaluation were performed. In cases of resected benign GPLs, eight were cholesterol polyps, and three were hyperplastic polyps. The other 8 cases of benign lesions were based on clinical follow-up at least one year after CEUS (mean observation time 37.1 months; range, 12.0–66.5 months). Patients with the following findings were excluded from this study: destruction of gallbladder wall by cancer invasion; and/or vessel and enhancement not visible due to artifacts from gallstones or intestinal gas. The institutional review board approved this study, and informed consent was obtained from all patients.

Equipment and protocol

The examinations were performed using LOGIQ 7 ultrasound systems equipped with two types of transducers, 3.5CS and 4D3CL (GE Healthcare, Ltd., Chicago, Illinois, USA). The 3.5CS probe was used for two-dimensional (2D) US and the 4D3CL, enabling mechanical sweep, was used for three-dimensional (3D) settings. Sonazoid contrast media was used for all patients. The same protocol was adopted for all examinations in B-mode and CEUS by 4 sonographers with CEUS experience of between 3 and 18 years (mean 8.8 years). Initially, all GPLs were scanned in B-mode with tissue harmonic imaging and size measured at the largest diameter. Subsequently, 0.2 mL of contrast agent was injected into the antecubital vein followed by bolus infusion of 2.5 mL of a 5% glucose solution. Contrast effect of whole GPL were obtained by manual or mechanical sweep immediately after injection of contrast agent for 120 s. The focus position was set just below the lesions and the high-MI contrast mode (i.e., CHA mode [MI = 0.8–1.2]) was used. Intermittent imaging (2 frames/s) was used for 2D US, and autosweep (8–13 frames/s) for 3D US. Data were stored on a hard disc of the US system and verified frame by frame after examination by each sonographer to choose static images of vessel(s) and enhancement in GPLs. The vessel images of GPL were evaluated between 10 and 50 s, and enhanced images were evaluated between 30 and 90 s after Sonazoid injection. Color Doppler images of GPL were not stored in all cases; therefore, we could not evaluate them in the present study.

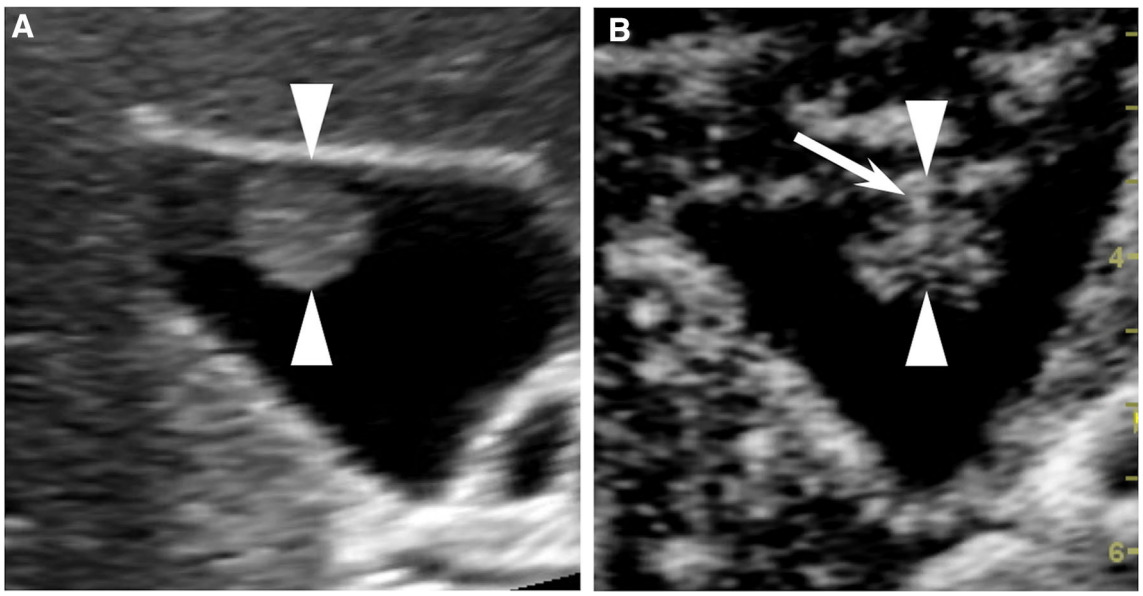

Fig. 2 Benign polypoid lesion of gallbladder (maximum diameter, 13 mm) in a 59-year-old woman. Arrowheads show margin of the lesion. **a** B-mode image reveals a hyper-echoic pedunculated polyp with smooth margin, homogeneous echogenicity, and hyper-echoic spot. **b** Contrast-enhanced ultrasound reveals a homogeneous and hypervascular pedunculated lesion. The thin and regular vessel in a stalk is clearly shown (arrow)

Image evaluation

All images were evaluated retrospectively by two readers with 10 and 7 years' experience evaluating CEUS images. The readers were blinded to the clinicopathological reports and other imaging findings. Evaluation criteria are explained in Fig. 1. In B-mode images, the readers evaluated echogenicity, morphology, outline, heterogeneity, and presence of hyperechoic spots. Echogenicity was classified by comparing the adjacent mucosal layer of gallbladder. Pedunculated lesions were defined as those having a pedicle or floating shape (Figs 2a, 4a); in contrast, a sessile lesion was defined as an elevated lesion with a broad base (Figs. 3a, 5a). Subsequently, both readers also

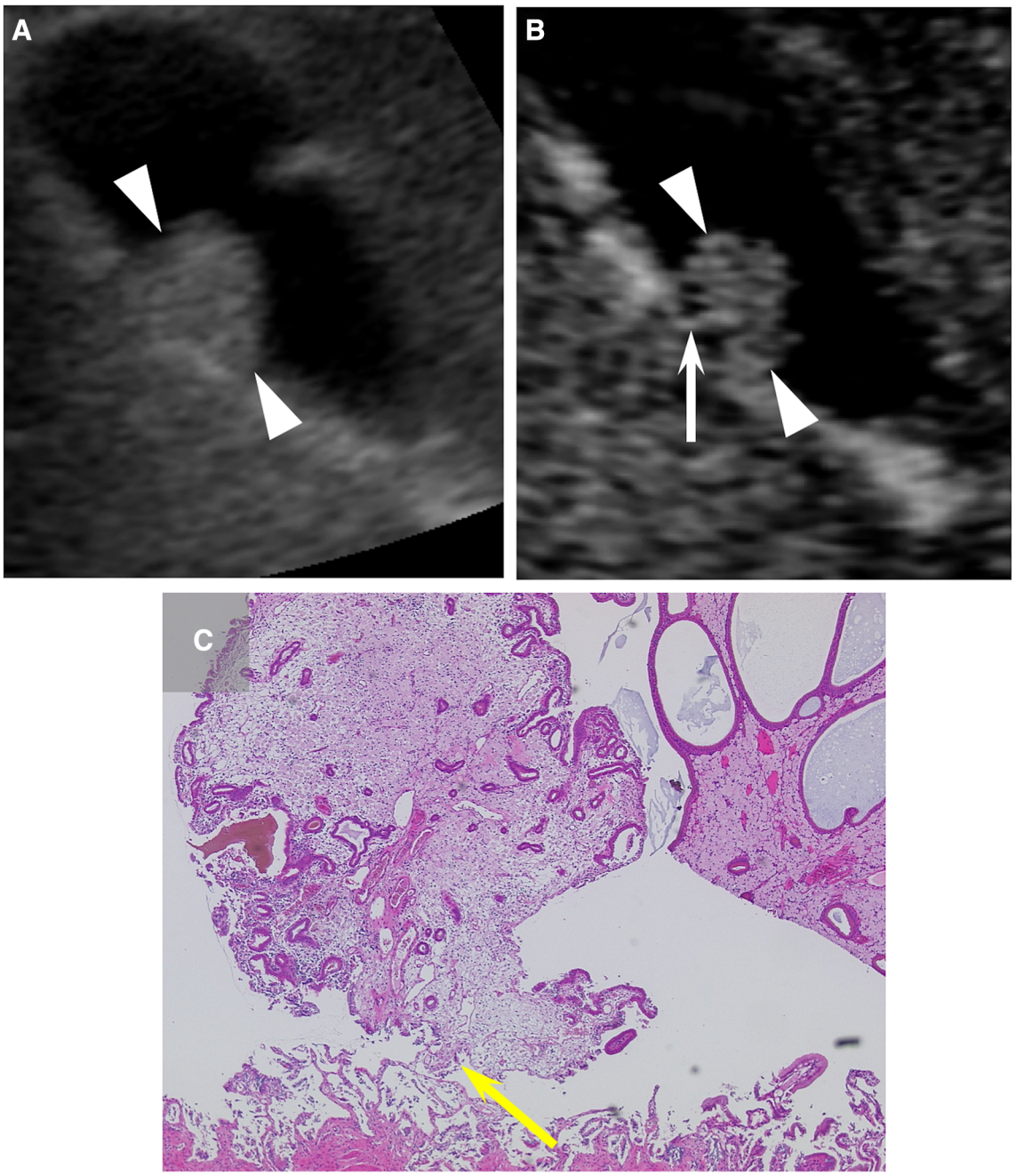

Fig. 3 Benign gallbladder polypoid lesion (maximum diameter, 10 mm) in a 55-year-old woman. Arrowheads show margin of the lesion. **a** B-mode image reveals a hyper-echoic sessile polyp with smooth margin and homogeneous echogenicity. Hyper-echoic spot is not shown; **b** Contrast-enhanced ultrasound image reveals a homogeneous and hypervascular pedunculated lesion with thin and regular single vessel in a stalk (arrow); **c** Histologic exam of the specimen reveals the polyp to be a cholesterol polyp with no dilated vessels at the stalk of lesion (arrow) (hematoxylin-eosin stain, × 40)

evaluated two still CEUS images that depicted vessels enhancement in the GPLs. The vessel images were clearly identified just before enhancement of the whole lesions, within 30 s of contrast media injection in most cases. Enhancement grade and heterogeneity were evaluated at the time of enhancement of whole lesions. They evaluated enhancement grade, morphology, vessel thickness, vessel shape, and heterogeneity of enhancement. Enhancement grade was classified into marked or mild enhancement. Regarding vessel thickness, we defined a vessel approximately ≥ 1 mm in width as dilated (Figs. 4b, 5b). Regarding vessel shape, orderly linear or spotty vessels were classified as regular (Fig 2b, 3b), and curved, tortuous and vessels were defined as irregular (Figs. 4b, 5b, 6b). The readers were trained using the definition and schema of each feature, and sample images of GPL on B-mode and CEUS before the image evaluation. Differences in findings between the two readers were finally resolved by consensus meeting.

Statistical analysis

Inter-observer agreement between the two blinded readers in each classification before consensus meeting was evaluated using the kappa statistic, graded as: poor (< 0.40); fair (0.40–0.60); good (0.60–0.80); or excellent (0.80–1.00). After consensus meeting, the clinical data and each finding in B-mode and CEUS were compared to evaluate differences between malignant and benign GPLs using the student *t*-test for continuous data and the chi-squared or Fisher's exact tests for categorical variables; a two-tailed $P < 0.05$ was considered to be statistically significant. The cut-off value of continuous data was obtained from the receiver operating characteristic (ROC) curve analysis. When multiple significant variables were identified, the number of features with the highest accuracy for malignant GPL was calculated. Sensitivity, specificity, and accuracy in B-mode and CEUS were calculated based on the diagnostic criteria, which were created from the results of the univariate analysis. Subsequently, a subgroup analysis was performed on the cases, in which there was no significant difference in the size of the GPLs, and the diagnostic value was also evaluated. All statistical analyses were performed using SPSS version 24 (IBM Corporation, Armonk, NY, USA).

Results

Characteristics of patients and GPLs

Patient characteristics are summarized in Table 1. Sex was not significantly different between patients with benign and malignant GPLs ($P = 0.739$). The mean age of patients with malignant GPLs was 72.4 ± 9.4 years (range, 52–87 years) and was significantly older than patients with benign GPLs (59.6 ± 12.3 years; range, 34–83) ($P < 0.001$). The mean size of malignant GPLs (23.4 ± 7.5 mm, range; 13–37 mm) was significantly larger than that of benign GPLs (12.4 ± 2.9 mm, range; 10–20 mm) ($P < 0.001$).

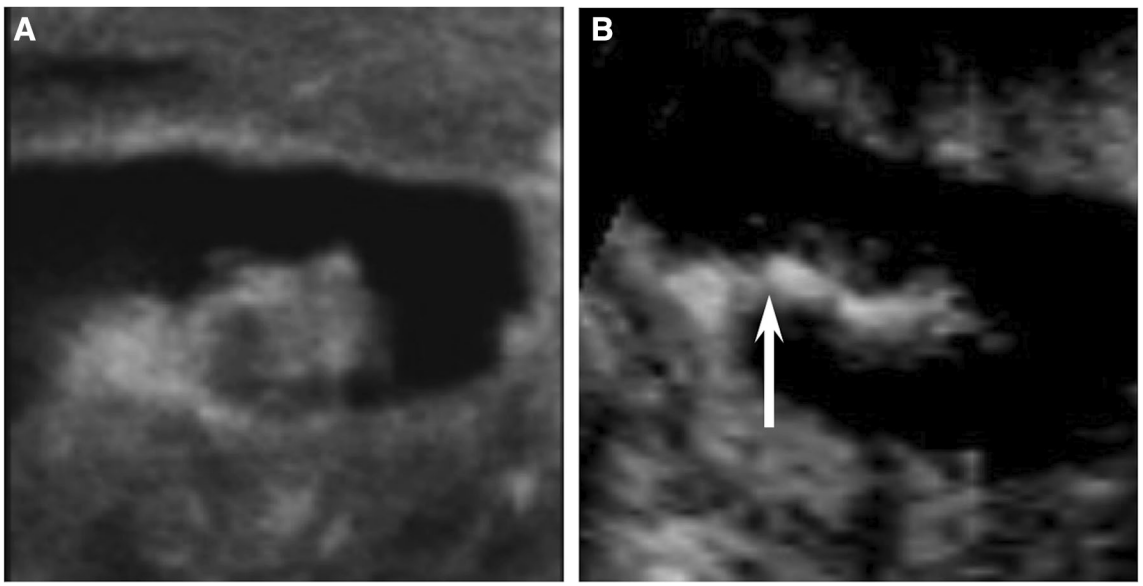

Fig. 4 Gallbladder cancer (maximum diameter, 17 mm) in a 66-year-old man. **a** B-mode image reveals a hyper-echoic pedunculated polyp, classified as unsmooth margin and heterogeneous. Stalk is shown on the left side of polyp (arrow); **b** Contrast-enhanced ultrasound image reveals a heterogeneous and hypervascular pedunculated lesion with dilated and irregular vessel (arrow)

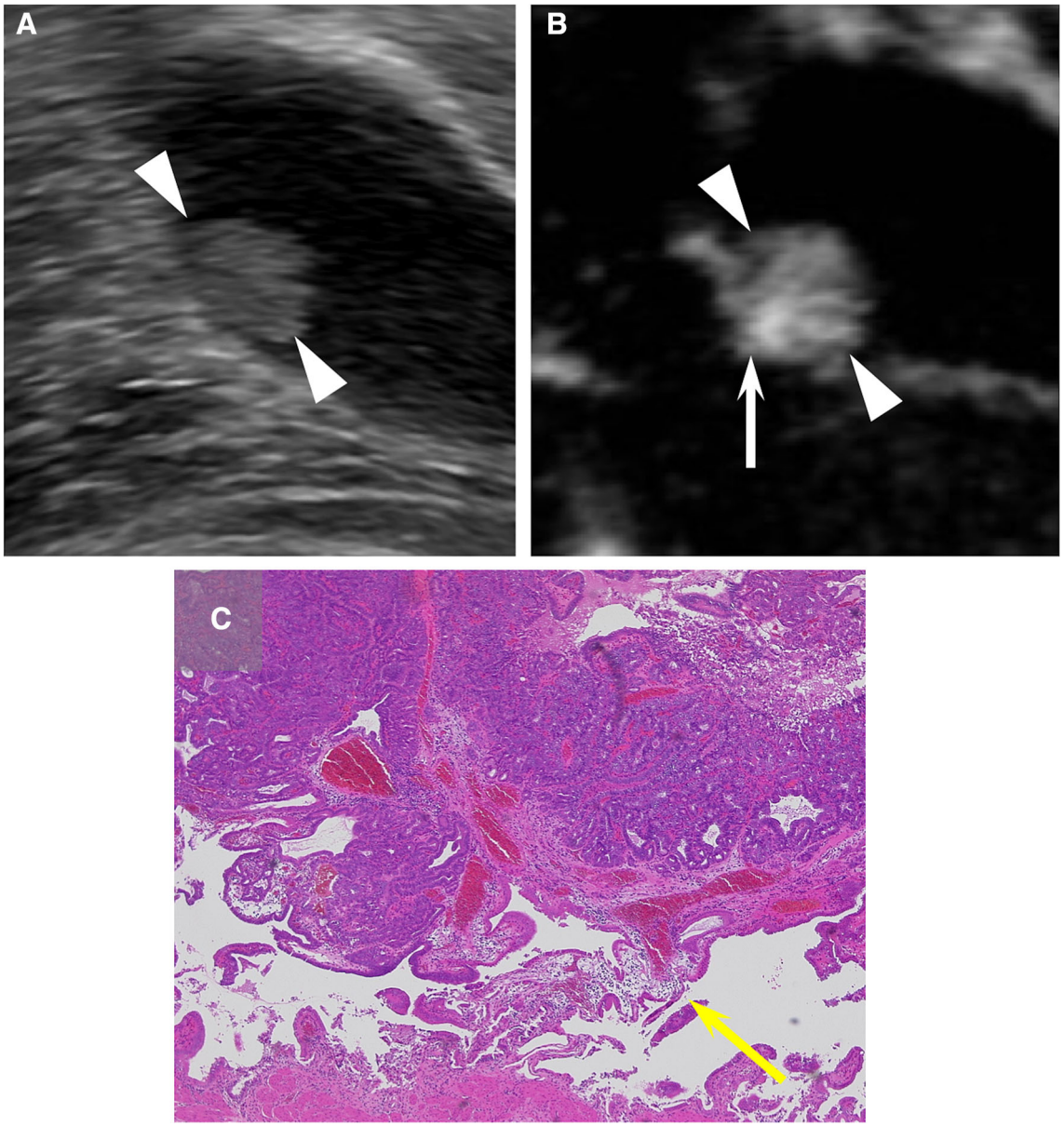

Fig. 5 Gallbladder cancer (maximum diameter, 13 mm) in a 52-year-old woman. Arrowheads show margin of the lesion. **a** B-mode image shows a hypo-echoic sessile polyp (arrowheads). It was classified as smooth margin and homogeneous echogenicity; **b** Contrast-enhanced ultrasound image reveals homogeneous and hypervascular pedunculated lesion with regular and dilated vessel in a stalk (arrow); **c** Histologic examination of the specimen reveals the polyp to be an adenocarcinoma with dilated vessels at the stalk of lesion (arrow) (hematoxylin-eosin stain, × 40)

Inter-observer agreement

Two malignant GPLs could not be evaluated due to a large amount of sludge and, were therefore, omitted from the evaluation in B-mode (Fig. 6). All findings observed in B-mode (34 cases) and CEUS (36 cases) by each of the two readers are summarized in Table 2. The findings confirmed by both readers achieved completely concordant results in 29% (10/34) in B-mode and 64% (23/36) on CEUS. The kappa values of findings in B-mode, echogenicity, morphology, outline, heterogeneity, and presence of hyperechoic spot(s), were 0.43, 0.64, 0.49, 0.41, and 0.54, respectively. Morphology of GPL was categorized as "good." and the other parameters are categorized as "poor" or "fair." On CEUS findings, the kappa value of enhancement grade, morphology of enhanced GPLs, vessel thickness, vessel shape, and heterogeneity of enhancement were 0.79, 0.83, 0.71, 0.66, and 0.82, respectively. All parameters on CEUS were categorized as "good" or "excellent."

Table 4 Accuracy of each diagnostic criteria

		Diagnostic criteria	Sensitivity	Specificity	Accuracy
	Age	> 65 years	88% (15/17)	68% (13/19)	78% (28/36)
	Size	> 16 mm	76% (13/17)	89% (17/19)	83% (30/36)
B-mode	Heterogeneity	Heterogeneous	80% (12/15)	68% (13/19)	74% (25/34)
CEUS	Morphology	Sessile	76% (13/17)	95% (18/19)	86% (31/36)
	Thickness of vessels	Dilated	71% (12/17)	89% (17/19)	81% (29/36)
	Shape of vessels	Irregular	82% (14/17)	95% (18/19)	89% (32/36)
	Heterogeneity	Heterogeneous	82% (14/17)	95% (18/19)	89% (32/36)
	Number of above 4 features on CEUS	One or more	94% (16/17)	89% (17/19)	92% (33/36)
		Two or more	88% (15/17)	95% (18/19)	92% (33/36)
		Three or more	65% (11/17)	95% (18/19)	81% (29/36)
		All	53% (9/17)	95% (18/19)	75% (27/36)

Findings after consensus meeting

Each category in B-mode and CEUS determined after consensus meeting are shown in Table 3. There was significantly different heterogeneity of the lesions in B-mode. Twelve (80%) cases of malignant GPLs and 6 (32%) cases of benign GPLs were heterogeneous ($P < 0.01$). There were no significant differences in other parameters in B-mode between benign and malignant GPLs. On CEUS, there was no significant difference in the enhancement grade between malignant and benign lesions. Other parameters, including morphology of enhanced GPLs, vessel thickness, vessel shape, and heterogeneity of enhancement, were significantly different (Figs. 2, 3, 4 5). Regarding morphology, 11 (58%) cases of benign GPLs laid on the gallbladder wall; therefore, they were mistakenly identified as sessile polyp with B-mode (Fig. 3a). However, on CEUS, ten cases of benign GPLs were observed as pedunculated polyps because the vessel in a stalk that attached to the gallbladder wall was clearly depicted (Fig. 3b). As a result, 13 (76%) cases of malignant GPLs were sessile polyps, in contrast, only one (5%) benign GPL had a sessile shape. Malignant GPLs had dilated (12/17 [71%]) and irregular (14/17 [82%]) vessels, and benign GPLs had thin (17/19 [89%]) and regular (18/19 [95%]) vessels. Heterogeneous enhancement was shown in 10 (59%) cases of malignant GPL and only one (5%) case of benign GPL.

Diagnostic value for malignant GPL

The accuracy of the diagnostic criteria for malignant GPL was summarized in Table 4. The cut-off values of patient age and lesion size for malignant GPL obtained from the ROC curve analysis were above 65 years and 16 mm, respectively. In B-mode, heterogeneous echogenicity was used in the diagnostic criterion for malignancy. On CEUS, there were four features that significantly correlated with malignant GPL by univariate analysis; and, the diagnostic criterion was defined as having one or more features. Sensitivity, specificity, and accuracy of the diagnostic criteria for malignant GPL were 88% (15/17), 68% (13/19), and 78% (28/36) for patient age; 76% (13/17), 89% (17/19), and 83% (30/36) for lesions size; 80% (12/15), 68% (13/19), and 74% (25/34) for B-mode; and 94% (16/17), 89% (17/19), and 92% (33/36) for CEUS, respectively.

Subgroup analysis

Table 5 summarizes the results of the subgroup analysis of the cases with the largest diameter of the GPL from 11 to 20 mm. This subgroup included 19 patients, eight with malignant GPLs and 11 with benign GPLs. There was no significant difference in the mean size of malignant (16.4 ± 2.8 mm) and benign (14.2 ± 4.0 mm) GPLs ($P = 0.402$). In B-mode, heterogeneous lesion was considerably higher in malignant GPLs, though the difference was not statistically significant ($P = 0.05$). In CEUS, sessile shape ($P < 0.01$), dilated vessels ($P < 0.05$), and irregular vessels ($P < 0.05$) were statistically significant for characterizing malignant GPL. The sensitivity, specificity, and accuracy of the diagnosis for malignant GPLs on CEUS were 88% (7/8), 91% (10/11), and 89% (17/19), respectively.

Discussion

Gallbladder lesions are classified into wall-thickening and polypoid lesions. Lesions with wall-thickening include gallbladder cancer, adenomyomatosis, chronic cholecystitis, and xanthogranulomatous cholecystitis [15], in contrast, GPLs include gallbladder cancer, adenoma, cholesterol polyp, hyperplastic polyp, and inflammatory

Table 5 Findings of GPLs within 11 to 20 mm after consensus meeting

	Malignant (N = 8)	Benign (N = 11)	P value
Characteristics			
Mean age ± SD (years)	73.5 ± 11.4	61.4 ± 10.0	0.463[a]
Mean size ± SD (mm)	16.4 ± 2.8	14.2 ± 4.0	0.402[a]
Female	50% (4/8)	36% (4/11)	0.658[b]
B-mode			
Echogenicity			1.000[b]
Hyperechoic	57 (4/7)	64 (7/11)	
Hypoechoic	43 (3/7)	36 (4/11)	
Morphology			0.630[b]
Sessile	57 (4/7)	36 (4/11)	
Pedunculated	43 (3/7)	64 (7/11)	
Outline			1.000[b]
Irregular	71 (5/7)	73 (8/11)	
Smooth	29 (2/7)	27 (3/11)	
Heterogeneity			0.050[b]
Heterogeneous	14 (1/7)	27 (3/11)	
Homogeneous	86 (6/7)	73 (8/11)	
Hyperechoic spots			0.627[b]
Absent	43 (3/7)	27 (3/11)	
Present	57 (4/7)	73 (8/11)	
CEUS			
Enhancement grade			0.228[b]
Marked	100 (8/8)	91 (10/11)	
Mild	0 (0/8)	9 (1/11)	
Morphology			0.006[b]
Sessile	75 (6/8)	9 (1/11)	
Pedunculated	25 (2/8)	91 (10/11)	
Thickness of vessel			0.041[b]
Dilated	38 (3/8)	91 (10/11)	
Thin	63 (5/8)	9 (1/11)	
Shape of vessels			0.041[b]
Irregular	38 (3/8)	91 (10/11)	
Regular	63 (5/8)	9 (1/11)	
Heterogeneity			0.262[b]
Heterogeneous	63 (5/8)	9 (1/11)	
Homogeneous	38 (3/8)	91 (10/11)	

GPLs Gallbladder polypoid lesions

Data are percentages; data in parentheses are numbers of the GPLs

One malignant GPL were omitted from B-mode images due to sludge

[a]According to the Student t-test

[b]According to the Fisher's exact test

polyp [16]. GPLs > 10 mm or growing in size have been reported to carry a risk for malignancy [5, 7, 8, 17]; however, benign GPLs are occasionally found to be > 10 mm in size [18]. In the present study, there were 19 benign GPLs ≥ 10 mm in size, and 58% (11/19) of patients underwent a cholecystectomy due to anxiety over malignancy, which was unnecessary. Therefore, we cannot differentiate GPLs based on the lesion size, even if it is a significant factor between benign and malignant GPLs. However, following-up these larger GPLs has the risk of overlooking gallbladder cancer in the early stage, and spreading by direct invasion or metastasis, even in a short period [19].

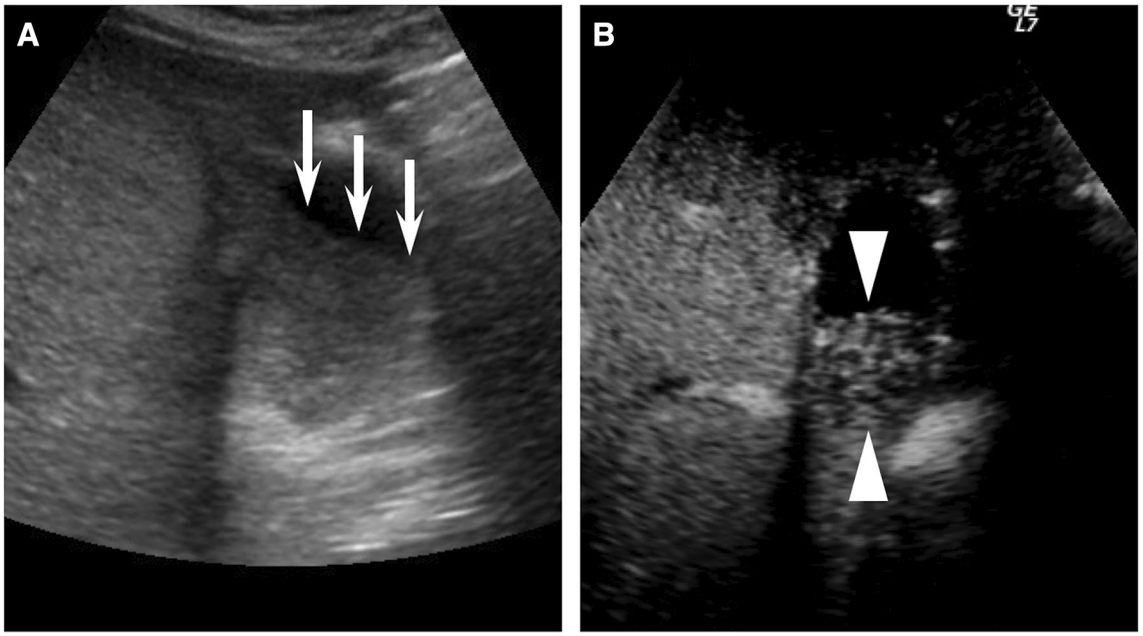

Fig. 6 Gallbladder cancer (maximum diameter, 26 mm) in a 75-year-old man. **a** B-mode image reveals only biliary sludge in a gallbladder. Arrows show margin of the sludge; **b** Contrast-enhanced ultrasound image can eliminate the background B-mode and reveal hypervascular sessile polyp with irregular vessel hidden by biliary sludge. Arrowheads show margin of the lesion

Regarding other risk factors, US findings of sessile-shape morphology were reported as one of the most important features of malignant GPLs [8]. However, in our study, 58% (11/19) of benign GPLs exhibited sessile shape in B-mode. The reason for this finding is considered that large pedunculated GPLs tend to lean against the gallbladder wall on account of their weight.

Features of echogenicity, outline of GPLs, and the presence of a hyperechoic spot cannot distinguish between malignant and benign GPLs in B-mode. Heterogeneous echogenicity was only the feature with a significant difference, indicating malignancy ($P < 0.01$), however, it lost statistical significance in subgroup analysis of lesion size within 11–20 mm at the largest diameter ($P = 0.050$).

Several investigators have reported the utility of CEUS using low-MI-contrast mode using SonoVue (Bracco, Milan, Italy), a microbubble contrast agent, for gallbladder lesions [20, 21]. However, comparing with contrast with the high-MI-contrast mode, low-MI-contrast mode cannot eliminate the background B-mode sufficiently. Then, it is difficult to evaluate the grade of vascularity and vessels running through the lesion and the stalk in details. Xiao et al evaluated enhancement grade by comparison with adjacent liver parenchyma [22]; however, the enhancement of liver parenchyma is often different among individuals according to the ultrasound attenuation due to thickness of skin surface or presence of fatty liver. Numata et al previously reported that all gallbladder lesions, except for sludge, exhibit vascularity [23]; therefore, it is necessary to find other features, except enhancement grade, for differential diagnosis of GPLs.

To improve the diagnostic accuracy of CEUS for GPLs, we adopted high-MI-contrast mode to eliminate background B-mode and obtain clear vessel images [24]. In this study, 71% (12/17) of malignant GPLs exhibited dilated vessels. Moreover, it enabled us to evaluate even minute linear vessels in the stalk(s) of benign GPLs, which are difficult to detect on color Doppler or CEUS using low-MI-contrast mode. According to the visualization of vessel in the stalks, 91% (10/11) of sessile GPLs in B-mode were classified as pedunculated lesions on CEUS. We believe CEUS with high-MI-contrast mode has greater advantage than color Doppler or CEUS with low-MI-contrast mode. Heterogeneity on CEUS was also an important feature, as previously reported [25, 26]. Moreover, the kappa value, which measures the inter-observer agreement, for CEUS (0.66–0.83) was superior to that for B-mode (0.41–0.61).

In this study, the diagnostic criteria for malignant GPL were defined from the results of the univariate analysis. To assess the diagnostic value of patient age and size of GPLs, the ROC analysis was used to calculate the cut-off value. In B-mode, heterogeneity was adopted as the diagnostic criterion for malignant GPL because it was the only feature significantly correlated with it. On CEUS, we have evaluated the number of features that would maximize the diagnostic accuracy for malignant GPL; thus, the diagnostic criterion was defined as having one or more of the following features: sessile shape, dilated vessel, irregular

vessel, or heterogeneous enhancement. According to these diagnostic criteria, sensitivity, specificity, and accuracy of the diagnosis of malignant GPL on CEUS were higher than that of patient age, size of GPL, and B-mode.

In the present study, malignant GPLs were significantly larger than benign GPLs; therefore, the abovementioned findings on CEUS may be influenced by the difference in size. To address this problem, we performed subgroup analysis for the cases having no significant difference in size of GPLs. In B mode, no feature had significant correlation with malignant GPLs, whereas, sessile shape, dilated vessels, and irregular vessels on CEUS showed significant difference between benign and malignant GPLs. The accuracy of diagnosing malignant GPLs between 11 and 20 mm in size suggested that CEUS was a useful modality in differentiating benign and malignant GPLs, regardless of their sizes.

Generally, morphological features and vessel images obtained using CEUS can aid in differentiating between malignant and benign GPLs. However, this study had several limitations, the first of which was its retrospective design. In cases of GPLs > 10 mm in size having apparent malignant findings such as peritonitis carcinomatosa, we did not perform CEUS. To avoid malignant GPLs, few cases of GPLs < 10 mm in seize were evaluated by CEUS and diagnosed as benign. However, we did not include them in this study due to the small number of cases. Therefore, we could not determine the ability of CEUS in diagnosing GPLs < 10 mm in size. Second, the number of enrolled patients with small malignant GPLs was lower than those with benign lesions. Third, in Japan, only Sonazoid is available as ultrasound contrast agent. Thus, we could not determine whether the CEUS findings of our study using Sonazoid in diagnosing GPLs were similar with those using other ultrasound contrast agents. Finally, 12 of 17 patients were diagnosed based on resected specimen. However, the remaining five patients with malignant GPLs were diagnosed based on pathological results, except those of resection. Moreover, we defined GPLs without growth over a one-year period as benign; however, it was possible that gallbladder adenomas, which grow slowly [27], were included in this study.

In conclusion, we classified the features of GPLs obtained by B-mode and CEUS, and the results of this study suggest that CEUS is a useful modality for differential diagnosis between malignant and benign GPLs.

Funding The present study did not receive any funding support.

Compliance with ethical standards

Conflict of interest All authors declare relevant conflicts of interest to disclose.

Ethical approval All procedures performed in studies involving human participants were in accordance with the ethical standards of the institutional and/or national research committee and with the 1964 Helsinki declaration and its later amendments or comparable ethical standards. The study was approved by the Yokohama City University Certified Institutional Review Board.

Informed consent Informed consent was obtained from individual participants included in the study.

References

1. Piehler JM, Crichlow RW (1978) Primary carcinoma of the gallbladder. Surg Gynecol Obstet 147:929–942
2. Naito Y, Okabe Y, Kawahara A, et al. (2009) Usefulness of lavage cytology during endoscopic transpapillary catheterization into the gallbladder in the cytological diagnosis of gallbladder disease. Diagn Cytopathol 37:402–406
3. Chantarojanasiri T, Hirooka Y, Kawashima H, et al. (2017) The role of endoscopic ultrasound in the diagnosis of gallbladder diseases. J Med Ultrason 44:63–70
4. Kozuka S, Tsubone N, Yasui A, Hachisuka K (1982) Relation of adenoma to carcinoma in the gallbladder. Cancer 50:2226–2234
5. Persley KM (2005) Gallbladder polyps. Curr Treat Options Gastroenterol 8:105–108
6. Lee KF, Wong J, Li JC, Lai PB (2004) Polypoid lesions of the gallbladder. Am J Surg 188:186–190
7. Boulton RA, Adams DH (1997) Gallbladder polyps: when to wait and when to act. Lancet 349:817
8. Bhatt NR, Gillis A, Smoothey CO, Awan FN, Ridgway PF (2016) Evidence based management of polyps of the gall bladder: a systematic review of the risk factors of malignancy. Surgeon 14:278–286
9. French DG, Allen PD, Ellsmere JC (2013) The diagnostic accuracy of transabdominal ultrasonography needs to be considered when managing gallbladder polyps. Surg Endosc 27:4021–4025
10. Zielinski MD, Atwell TD, Davis PW, Kendrick ML, Que FG (2009) Comparison of surgically resected polypoid lesions of the gallbladder to their pre-operative ultrasound characteristics. J Gastrointest Surg 13:19–25
11. Song ER, Chung WS, Jang HY, Yoon M, Cha EJ (2014) CT differentiation of 1-2-cm gallbladder polyps: benign vs malignant. Abdom Imaging 39:334–341
12. Watanabe R, Matsumura M, Chen CJ, Kaneda Y, Fujimaki M (2005) Characterization of tumor imaging with microbubble-based ultrasound contrast agent, sonazoid, in rabbit liver. Bio Pharm Bull 28:972–977
13. Luo W, Numata K, Morimoto M, et al. (2009) Clinical utility of contrast-enhanced three-dimensional ultrasound imaging with Sonazoid: findings on hepatocellular carcinoma lesions. Eur J Radiol 72:425–431
14. Miwa H, Numata K, Sugimori K, et al. (2014) Differential diagnosis of solid pancreatic lesions using contrast-enhanced three-dimensional ultrasonography. Abdom Imaging 39:988–999
15. Runner GJ, Corwin MT, Siewert B, Eisenberg RL (2014) Gallbladder wall thickening. Am J Roentgenol 202:W1–w12
16. Mellnick VM, Menias CO, Sandrasegaran K, et al. (2015) Polypoid lesions of the gallbladder: disease spectrum with pathologic correlation. Radiographics 35:387–399
17. Wiles R, Thoeni RF, Barbu ST, et al. (2017) Management and follow-up of gallbladder polyps : Joint guidelines between the European Society of Gastrointestinal and Abdominal Radiology (ESGAR), European Association for Endoscopic Surgery and other Interventional Techniques (EAES), International Society of

Digestive Surgery - European Federation (EFISDS) and European Society of Gastrointestinal Endoscopy (ESGE). Eur Radiol 27:3856–3866
18. Kimura K, Fujita N, Noda Y, Kobayashi G, Ito K (2001) Differential diagnosis of large-sized pedunculated polypoid lesions of the gallbladder by endoscopic ultrasonography: a prospective study. J Gastroenterol 36:619–622
19. Kondo S, Nimura Y, Kamiya J, et al. (2002) Mode of tumor spread and surgical strategy in gallbladder carcinoma. Langenbecks Arch Surg 387:222–228
20. Xu JM, Guo LH, Xu HX, et al. (2014) Differential diagnosis of gallbladder wall thickening: the usefulness of contrast-enhanced ultrasound. Ultrasound Med Biol 40:2794–2804
21. Negrao de Figueiredo G, Mueller-Peltzer K, Zengel P, et al. (2018) Diagnostic performance of contrast-enhanced ultrasound (CEUS) for the evaluation of gallbladder diseases. Clin Hemorheol Microcirc 69:83–91
22. Xie XH, Xu HX, Xie XY, et al. (2010) Differential diagnosis between benign and malignant gallbladder diseases with real-time contrast-enhanced ultrasound. Eur Radiol 20:239–248
23. Numata K, Oka H, Morimoto M, et al. (2007) Differential diagnosis of gallbladder diseases with contrast-enhanced harmonic gray scale ultrasonography. J Ultrasound Med 26:763–774
24. Numata K, Luo W, Morimoto M, et al. (2010) Contrast enhanced ultrasound of hepatocellular carcinoma. World J Radiol 2(2):68–82
25. Choi JH, Seo DW, Choi JH, et al. (2013) Utility of contrast-enhanced harmonic EUS in the diagnosis of malignant gallbladder polyps (with videos). Gastrointest Endosc 78:484–493
26. Kamata K, Takenaka M, Kitano M, et al. (2018) Contrast-enhanced harmonic endoscopic ultrasonography for differential diagnosis of localized gallbladder lesions. Dig Endosc 30:98–106
27. Yuan HX, Cao JY, Kong WT, et al. (2015) Contrast-enhanced ultrasound in diagnosis of gallbladder adenoma. Hepat Pancreat Dis Int 14:201–207